Multiphoton absorption in germanium using pulsed infrared free-electron laser radiation

D. Seo, J. M. Gregory, L. C. Feldman, N. H. Tolk, and P. I. Cohen

Phys. Rev. B **83**, 195203 — Published 4 May 2011

DOI: 10.1103/PhysRevB.83.195203

Multiphoton absorption in germanium using pulsed IR FEL radiation

D. Seo,[1,2] J. M. Gregory,[2] L. C. Feldman,[2,3] N. H. Tolk,[2] P. I. Cohen[1,*]

[1]*Department of Electrical and Computer Engineering, University of Minnesota, Minneapolis, MN 55455, USA.*

[2]*Department of Physics and Astronomy, Vanderbilt University, Nashville, TN 37235, USA*

[3]*Institute of Advanced Materials, Devices and Nanotechnology, Rutgers, The State University of New Jersey, Piscataway, NJ 08854, USA*

ABSTRACT

We report wavelength- and intensity-dependent transmission measurements of intense mid-infrared radiation from the Vanderbilt Free Electron Laser in single-crystal Ge(100) in the wavelength range of 2.8–5.2 μm. This range accesses both the direct and indirect energy gaps in Ge, requiring in each case either two or three photons (2PA or 3PA) for absorption. Large changes in the multi-photon absorption rate are seen at the direct-to-indirect and 2PA-to-3PA transitions. Photon interactions are dominated by free carrier absorption (FCA), primarily due to holes. The entire absorption process is modeled with the two- and three-photon absorption coefficients (β and γ) as fitting parameters. Using newly measured values of the low-intensity FCA cross-sections, we find a best fit to the data at 2.8 μm that is in agreement with theory and previous measurements. We report a ratio of 175 for β across the direct-to-indirect transition, and a ratio of 5 across the same transition for γ. These ratios are independent of systematic variations in free carrier cross-sections and beam diameter.

Receipt Date: Oct. 8, 2010

PACS: 78.20.Bh, 78.20.Ci, 79.20.Ws

Keywords: mid-infrared, transmittance, germanium, free electron laser, two-photon absorption, three-photon absorption, and nonlinear process.

I. INTRODUCTION

The incidence of high-power and ultra-fast electromagnetic radiation on materials results in an array of complex laser-material interactions.[1-3] Laser-induced heating,[4] melting,[5] laser ablation,[6] shock wave dynamics,[7] Coulomb explosions,[8] and plasma formation[9] are typical examples. Laser-material interactions are heavily dependent on laser beam parameters such as pulse duration, intensity, and wavelength, as well as on material properties such as the band gap for semiconductors and dielectrics.[10] The determination of photon energy absorption mechanisms in transparent materials where $\hbar\omega < E_g$ is a fundamental issue. In this paper we report on the interaction of intense mid-infrared (IR) radiation in single-crystal germanium (Ge) where the incident photon energy is well below the band gap energy.

Germanium is an important group IV semiconducting material. Its unique physical properties—such as its high index of refraction and transparency in the IR—give rise to important applications in optics and electronics (*e.g.*, lenses, windows, IR detectors, fibers, and high speed integrated circuits). In addition, Ge is one of only a few common semiconductors where indirect and direct absorption regimes can be accessed at comparable wavelengths. However, there have been relatively few fundamental studies of the nonlinear optical properties of Ge undergoing high-power mid-IR irradiation,[11-18] in part due to the scarcity of appropriate sources. In this work we employ the Vanderbilt University Free Electron Laser (FEL), one of the most intense sources available for such investigations.

Direct two-photon absorption (2PA) in germanium at wavelengths ranging from 2.6 μm to 3.0 μm was studied by Gibson *et al* in 1976 using a hydrogen fluoride laser.[12] In 1980, Yuen *et al* used a CO_2 laser at fixed wavelengths of 9.6 μm and 10.6 μm.[18] Multiphoton absorption was proposed as the explanation for the observed saturation in the transmission in their report. In addition, free carrier absorption and impact ionization were proposed as possible absorption mechanisms in an earlier theoretical paper.[13] Indirect two-photon absorption in Ge was first observed in 1993 utilizing the Vanderbilt University FEL.[16] In 1997, multiphoton absorption at 2.9 μm was reported by Rauscher and Laenen.[14] More recently, a study of the interaction between crystalline Ge and mid-IR (λ = 5.3–12.4 μm) radiation, using the Osaka University FEL, was reported.[11, 19, 20] Finally, a recent PhD dissertation[17] has studied multiphoton absorption and damage thresholds in Ge at 2.05 μm and 2.5 μm.

One notable wavelength range missing from the works listed above is the 3.0–5.2 μm regime, for which the FEL at Vanderbilt University is well suited. In this study, we measure multiphoton absorption coefficients for Ge in the mid-IR, ranging from λ = 2.8 μm to 5.2 μm, a range in which we observe both two- and three-photon absorption, in each case across both the direct and indirect gaps.

II. EXPERIMENTAL DETAILS

The Vanderbilt University FEL provides a high-power beam in the mid-IR from 2–9 μm.[21] The beam comes in a train macropulses, each consisting of approximately 14,000 one-ps micropulses with 350 ps separation. A macropulse extends for about 5 μs with a repetition rate of 30 Hz. These pulse structures are shown schematically in Figs. 1(a) and 1(b). The macropulse-to-macropulse energy fluctuations were a source of random error, typically ± 5%, and the error became smaller as higher macropulse energies were used. For example, 1 ± 0.05 mJ and 10 ± 0.2 mJ were observed. Micropulse-to-micropulse fluctuations were less than 10%.[22] The micropulses were nearly transform-limited as measured by autocorrelation, and were assumed to have a Gaussian temporal profile. Although individual micropulse chirping was minimal, the wavelength of the micropulses could vary over the course of the macropulse by as much as 50 nm for the shorter wavelengths studied and as much as 100 nm for the longer wavelengths. Spatially, the FEL beam profile was very near to Gaussian.

The linearly polarized FEL output energy was adjusted using a rotating Brewster's angle Ge attenuator, and the radiation was focused onto a Ge sample using a ZnSe lens with 250 mm focal length. (In polarization experiments with this apparatus, the absorption showed no measurable dependence on incident polarization). Incident and transmitted laser energies were measured respectively with and without the sample using a power meter, as depicted in Fig. 1(c).

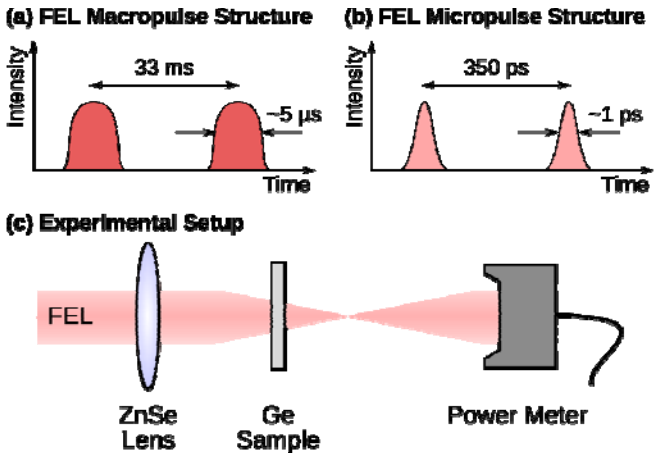

FIG. 1. FEL pulse structure and experimental setup. (a) The pulse duration of a macropulse is 5 μs with a repetition rate of 30 Hz. (b) Each macropulse consists of a train of 14,000 micropulses of 1 ps duration, separated by 350 ps. (c) A schematic diagram of the experimental setup.

We note that during the 350 ps between FEL micropulses, it is expected that photo-generated carriers will have sufficient time to relax to the lowest level excited states, including the relaxation of Γ valley electrons to the L valley, but not enough time to undergo any substantial recombination, even at the very high concentrations generated. The 33 ms between macropulses is sufficient for the entire electronic system to recover to the ground state via recombination, with essentially no excited carriers remaining. Because of its pulse structure, the FEL is a unique photon source, substantially different from conventional tabletop laser sources.

Double-side polished, 0.5 mm-thick near-intrinsic n-type Ge(100) samples were used. The samples had a resistivity of ~ 50 Ω • cm, corresponding to a free carrier concentration in the range of 10^{13}–10^{14} cm^{-3}. All experiments were performed in air at room temperature. Fourier transform infrared (FTIR) measurements were also performed to establish the low-power transmittance of the samples at the wavelengths studied.

For all wavelengths studied, strong nonlinear absorption and material removal (ablation) were observed whenever the sample was placed at the focal point, even at low macropulse energies (E_M < 3 mJ).[15] Therefore, transmission was measured at all wavelengths with the sample at a fixed distance of 24 cm from the lens, away from focal point, permitting the use of higher macropulse energies (up to 30 mJ) and increasing the range of incident intensities in the experiment.

As will be discussed in Section IV, the beam diameter at the sample and the free carrier absorption coefficients are critical values in the characterization of nonlinear interactions between the samples and the FEL beam. We will first discuss the beam diameter. We used a *z*-scan technique to determine the focal point of our lens at different wavelengths, as shown in Fig. 2(a). The focal length was found to increase linearly with increasing wavelength. Since the FEL beam diameter does not vary significantly with wavelength, we assume a linear relationship between the beam wavelength and the beam diameter at the fixed sample position. FWHM beam diameters at the sample position for 2.8 μm and 5.2 μm were determined by setting the incident beam fluence to twice the damage threshold for those wavelengths and then measuring the diameters of the resultant damage spots (see Fig. 2(b)). The beam diameters for the intermediate wavelengths were then interpolated, as shown in Fig 2(c). This "damage spot" method was found to be in agreement with the result of the knife-edge method in a comparison of the two at the focal point.

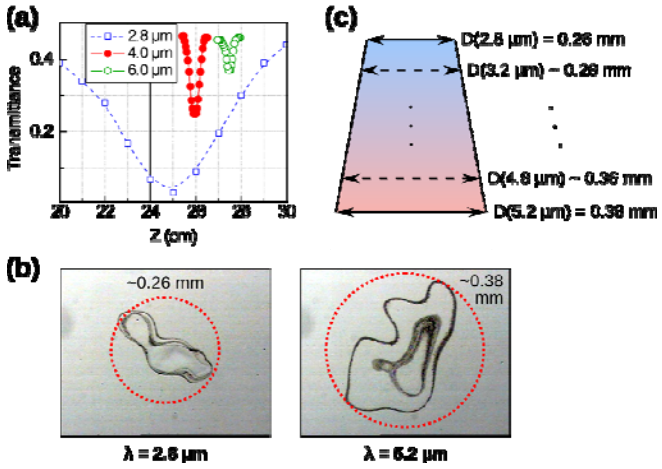

FIG. 2. Beam diameter determination using *z*-scan and optical microscopy. (a) *z*-scans for 2.8 μm, 4.0 μm, and 6.0 μm. Transmission for all wavelengths was measured at a fixed sample position, as marked by the dark line. (b) Optical microscopy images of surface-damaged Ge. Measured beam diameters of 0.26 mm at 2.8 μm (left) and 0.38 mm at 5.2 μm (right), as marked by the dotted circles. Irregularities in the spots may be attributed to damage nucleation mechanisms in addition to irregularities in the FEL beam. (c) Beam diameters at the sample for wavelengths ranging from 3.2 μm to 4.8 μm were interpolated linearly using the measurements shown in (b).

To determine the wavelength-dependent free carrier absorption coefficients σ_n (electrons) and σ_p (holes), we measured the FTIR spectra of heavily doped n-type ($N_n \sim 7 \times 10^{17}$ cm^{-3}) and p-type ($N_p \sim 2.5 \times 10^{16}$ cm^{-3}) Ge samples, and compared them to the spectrum for the near-intrinsic sample. The results are summarized in Table 1. The values at 2.8 μm are comparable to previously reported measurements.[23] Since the majority of free carriers encountered by the photons in the FEL beam will have relaxed to the band edge,[24] we believe that this method provides realistic absorption coefficients for our experiment.

TABLE I. Absorption cross-sections in Ge for electrons (σ_n) and holes (σ_p) as measured by low-intensity FTIR.

λ (μm)	σ_n (10^{-17} cm^2)	σ_p (10^{-16} cm^2)
2.8	0.72	1.4
3.2	0.78	1.5
3.6	0.87	1.3
4.0	0.95	0.95
4.4	1.06	0.8
4.8	1.17	1.0
5.2	1.32	0.7

III. RESULTS

Figure 3 shows transmittance as a function of incident micropulse peak intensity for wavelengths ranging from 2.8 μm to 5.2 μm, at 0.4 μm intervals. The measured incident macropulse energy E_M was converted into the micropulse peak intensity I_μ according to the following equation:

$$I_\mu = \frac{E_M/14000}{\pi^{3/2} r_0^2 t_0}, \tag{1}$$

where r_0 is the HWe^{-1}M beam radius and t_0 is the HWe^{-1}M micropulse length (HWe^{-1}M = FWHM / 1.66511). We note at the outset that at 4.0 μm, the low-intensity limit did not approach the FTIR limit as expected, rendering suspect the result at that wavelength. We believe this anomaly was due to instability in the FEL beam during measurement.

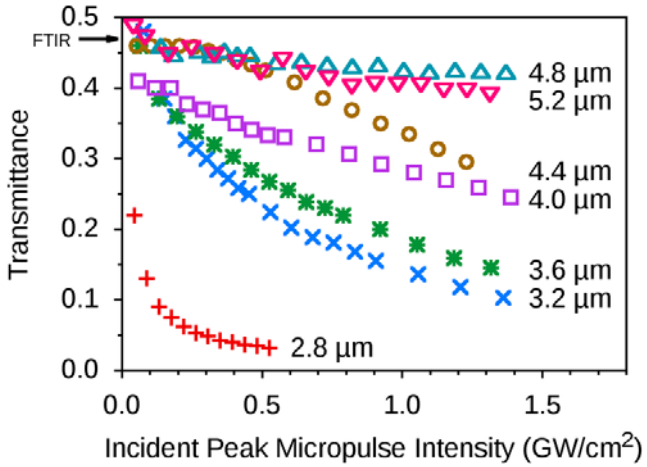

FIG. 3. Transmittance as a function of incident micropulse peak intensity for the seven different wavelengths studied. FTIR on the Ge sample shows a transmittance of 0.47 at low power (black arrow, upper left).

The data separate into four groups at high intensity, with a general trend of decreased absorption for higher-order processes. The fast transmittance decrease at 2.8 µm (0.44 eV) as a function of incident intensity is attributed to two-photon absorption across the direct band gap (~0.8 eV). The intermediate decrease at 3.2 µm (0.39 eV) and 3.6 µm (0.34 eV) is attributed to 2PA across the indirect band gap (0.66 eV). We attribute the relatively slow transmittance decrease at 4.0 µm (0.31 eV) and 4.4 µm (0.28 eV) to direct three-photon absorption (3PA), and the small decrease in transmittance observed at 4.8 µm (0.26 eV) and 5.2 µm (0.24 eV) to indirect 3PA.

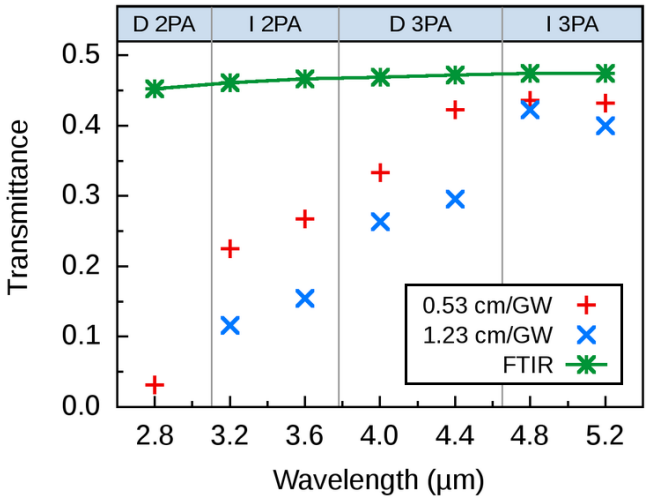

FIG 4. Transmittance cross-sections at two incident peak intensities, showing wavelength dependence, along with the low-intensity FTIR transmittance. The attributed absorption regimes (direct 2PA, etc.) are noted at the top of the plot.

Figure 4 shows the same data as a function of wavelength at two different intensities, highlighting the dramatic change in transmittance between the various absorption regimes. These differences are especially clear in the high-intensity (1.23 cm/GW) curve. The low-intensity FTIR transmittance is also shown, for comparison.

IV. DISCUSSION

A. Computational Model

The transmission curves shown above were analyzed using the following theoretical model. The nonlinear absorption of optical pulses at sub–band-gap wavelengths may be described by the equation:

$$\frac{\partial I}{\partial z} = -\beta I^2 - \gamma I^3 - (\sigma_n + \sigma_p) N I, \tag{2}$$

where I is the intensity of the pulse as a function of space and time, β is the two-photon absorption coefficient (units cm/GW), γ is the 3PA coefficient (cm^3/GW^2), and the last term describes free carrier absorption. The time evolution of the local free carrier concentration N is described as:

$$\frac{\partial N}{\partial t} = \frac{\beta I^2}{2\hbar\omega} + \frac{\gamma I^3}{3\hbar\omega} + D\frac{\partial^2 N}{\partial z^2} - \frac{N}{\tau} - AN^3. \tag{3}$$

Here the first and second terms refer to two- and three-photon absorption, respectively, with $\hbar\omega$ as the energy of the absorbed photons. The third term refers to free carrier diffusion with ambipolar diffusion coefficient $D = 67$ cm^2/s,[25] the fourth term to radiative recombination with lifetime $\tau = 100$ μs,[26] and the final term to Auger recombination with Auger coefficient $A = 2 \times 10^{-31}$ cm^6/s.[27, 28]

This pair of coupled differential equations was solved numerically using a time-and-space–discreet pulse propagation simulation, with consideration given to the profile of the micropulses in time and space (assumed to be Gaussian in both cases), multiple reflections inside the sample using the usual Fresnel coefficients, and to the accumulation of carriers between micropulses. The simulation code was verified for accuracy by comparison with simpler analytical models. We have considered the possible effects of surface recombination, temperature rise due to carrier relaxation, and bleaching due to relaxed state filling and have found them all to be negligible.

B. Beam Propagation and Carrier Concentrations

The simulations provide information about pulse intensity and carrier concentration throughout the sample depth. For instance, when the absorption was low, which occurred at low incident intensities for the shorter wavelengths and at all intensities for the longer wavelengths, a relatively even carrier distribution was produced. In these cases, the micropulses tended to lose their energy gradually as they traversed the sample. At the weakest intensity for 2.8 μm, for example, after the complete macropulse had traversed the sample, the carrier concentration near the front surface was 1.1×10^{18} cm^{-3} and decayed exponentially toward the back surface, where it was 2×10^{17} cm^{-3}.

When the absorption was high, as in the high-intensity, shorter-wavelength case, the micropulses tended to lose most of their energy quickly upon entering the sample, resulting in greater carrier concentrations near the front surface. For example, after the highest-intensity 2.8 μm macropulse had traversed the sample, the front surface carrier concentration was 6×10^{18} cm^{-3}, and decayed exponentially to a back surface carrier concentration of 2×10^{17} cm^{-3}, as in the low-absorption case.

In either case, for a given FEL macropulse, the carrier concentrations increased steadily with each micropulse until competition with recombination processes caused the system to approach a quasi-steady state. In the high-absorption regime, this state was reached after a few hundred micropulses. In the low-absorption regime, several thousand were required to reach it, or it was not

reached at all. For instance, at the highest intensity studied for 4.8 μm, the carrier concentration never reached steady state, and was ~2×10^{16} throughout the entire sample depth at the end of the macropulse.

TABLE II. Fitted absorption coefficients for the transmission data shown in Fig. 3. For 2PA, $x = 2\hbar\omega/E_g$, where E_g may refer to either the direct (0.8 eV) or indirect (0.67 eV) gap. For 3PA, $x = 3\hbar\omega/E_g$.

λ (μm)	Abs. Type	x	Fitted Coefficient
2.8	D 2PA	1.11	$\beta = 30.$ cm/GW
3.2	I 2PA	1.17	$\beta = 0.16$ cm/GW
3.6	I 2PA	1.04	$\beta = 0.090$ cm/GW
4.0	D 3PA	1.16	$\gamma = 0.27$ cm^3/GW^2
4.4	D 3PA	1.06	$\gamma = 0.067$ cm^3/GW^2
4.8	I 3PA	1.16	$\gamma = 0.0050$ cm^3/GW^2
5.2	I 3PA	1.07	$\gamma = 0.013$ cm^3/GW^2

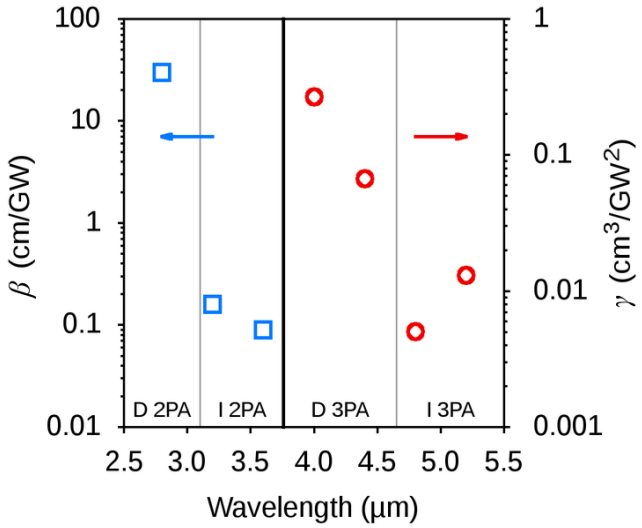

FIG 5: Fitted absorption coefficients for the transmission data shown in Fig. 3. The squares are 2PA coefficients (left axis) and the circles are 3PA coefficients (right axis).

C. Absolute Nonlinear Absorption Coefficients

Table II lists the fitted absorption coefficients β and γ for the wavelengths studied. The same coefficients are plotted in Fig. 5. In the 2PA data, there is a distinct change in the absorption

coefficients between the direct and indirect regimes. In the 3PA data, this difference is not so pronounced. The decreased absorption in the indirect regimes is reasonable considering the need for phonon assistance in exciting carriers to the indirect valley. In addition, the less pronounced difference in the 3PA data may be attributed to the greater number of absorption pathways generally available in 3PA, as recently shown by Cirloganu et al.[29]

TABLE III. Selected literature values for β in Ge near 2.8 μm, along with the result of the current work.

Work	Year	λ (μm)	β (cm/GW)
Gibson[12]	1976	2.6—3.0	160
Rauscher[14]	1997	2.9	80
Wagner[17]	2010	2.5	68
Current	2010	2.8	30

Previous works have reported the 2PA coefficient in Ge near 2.8 μm. These are listed in Table III, and are in the same range as our result. The derived value of β at 2.8 μm (30 cm/GW) is a factor of five less than the earliest observations at similar wavelengths[12], and is a factor of two less than the more recent measurements.[14, 17] We have also compared our results to predictions based on Wherrett's scaling rule,[30] which has been remarkably successful in predicting the nonlinear behavior of a variety of direct-gap materials.[31] At 2.8 μm, Wherrett scaling predicts $\beta = 40.9$ cm/GW, which is consistent with our result, and is evidence that multiphoton absorption theory for direct-gap materials is applicable to direct transitions in indirect-gap materials. For the direct 3PA wavelengths we find that the Wherrett scaling overestimates the coefficients by factors of 40 for 4.0 μm and 225 for 4.4 μm. However, recent theoretical results[32] have shown that more complex models are necessary to accurately describe 3PA behavior. Finally, although important theoretical steps have been made in addressing 2PA and 3PA in indirect-gap materials,[33] more theoretical work is needed in this area before quantitative comparisons can be made between experimental and theoretical results.

The coefficients listed in Table II are subject to a few caveats. One is due to the uncertainty in the beam area at the sample. We have used interpolated values for the beam diameter, as described in Section II. Errors in beam diameter measurement affect the incident pulse intensity by Eq. 1, with the result that the data in Fig. 3 may be scaled horizontally along the intensity axis. In addition, the fitting simulations used a Gaussian spatial profile, but the FEL beam has some spatial irregularities.

We find that a 10% variation in the beam diameter can result in a 50% variation in the derived coefficients.

The second major caveat is due to uncertainty in the free carrier absorption cross-sections. Free carriers generated by multiphoton absorption can be excited further by single-photon absorption, either due to subsequent photons in the same micropulse or in latter micropulses. Ignoring free carrier absorption effects can cause derived multiphoton absorption coefficients to be off by orders of magnitude.[12, 34] While in other works the 2PA/3PA coefficients and free carrier cross-sections are fitted simultaneously,[35] in this work we have used FTIR of doped samples to measure these values directly, as described in Section II. Still, these cross-sections may be influenced by a variety of factors, and in particular the energy state of the photo-excited carrier undergoing absorption, though as discussed earlier the unique pulse structure of the FEL should allow sufficient time for carrier relaxation, more than other laser sources. Nevertheless, we note that a 10% variation in the free carrier absorption cross-sections σ_n and σ_p can result in a 15% variation in the derived multiphoton absorption coefficients.

D. Ratio of Absorption Coefficients: Direct to Indirect

Although the caveats listed above, which are common to nonlinear absorption experiments, cast some uncertainty on the reported absolute absorption coefficients, we find that the ratios of these coefficients across the direct-to-indirect transitions for 2PA and 3PA are invariant to systematic changes of at least 20% in both beam diameter and free carrier absorption coefficients. Essentially all theoretical treatments of nonlinear absorption consider a multiplicative factor $f(x) \geq 0$ that reflects the multiple ways that two or three photons can add to give multiphoton absorption. For 2PA, $x = 2\hbar\omega/E_g$, and for 3PA, $x = 3\hbar\omega/E_g$. (Here, E_g may refer to the direct (0.8 eV) or indirect (0.67 eV) gap, depending on the absorption regime.) Ideally, comparisons of ratios across the direct/indirect transitions should be made using the same value of x. For the 2PA ratio, we have used 2.8 μm ($x = 1.11$) and 3.2 μm ($x = 1.17$). For 3PA, we have used 4.4 μm ($x = 1.06$) and 5.2 μm ($x = 1.07$). For the transition from 2.8 μm to 3.2 μm, we find a ratio in β of 175. In a previous work[16] this ratio was estimated as 2,000. For the transition from 4.4 μm to 5.2 μm, we find a ratio in γ of 5. These ratios should prove valuable in the continued development of the theoretical models for indirect 2PA and 3PA. A comparison of two separate experiments in silicon[36, 37] shows a ratio of 17 across the

2PA direct/indirect transition. We emphasize the advantage in this work of using a single laser source and experimental setup for all wavelengths.

E. Ratio of Absorption Coefficients: 2PA to 3PA

A comparison of $\beta / \gamma I$ provides a measure of the relative importance of 2PA to 3PA at a given intensity I. Assuming that the direct 3PA remains on the order of 0.05 cm^3/GW^2 in the wavelength regimes were 2PA is allowed, we find that at 2.8 μm 3PA will dominate at intensities greater than 300 GW/cm^2. For 3.2 μm and 3.6 μm, 3PA will dominate above ~2.5 GW/cm^2.

F. Ratio of Absorption Coefficients: 3.2 μm to 3.6 μm

The theoretical work of Garcia and Kalyanaraman on indirect 2PA in silicon[33] predicts the relative indirect absorption coefficients at different wavelengths. Although their work dealt with silicon, the general shape of the curve as a function of x should hold for other materials. At 3.2 μm and 3.6 μm, the Garcia theory predicts that the allowed-allowed transition dominates and calculates a ratio of 10 between the coefficients at these wavelengths. In this work, we find a ratio of 2.

V. SUMMARY

The wavelength- and intensity-dependent transmission of intense mid-infrared radiation in single-crystal Ge(100) is reported. The data show strong nonlinear intensity dependence and a strikingly large variation in absorption across a narrow range of wavelengths. Absorption coefficients and the first quantitative ratios across direct and indirect regimes for Ge are reported. These new results extend the investigated region of nonlinear absorption in Ge, and their interpretation provides insight into the complex mechanisms involved. These results not only reveal the fundamental mechanisms associated with such processes, but also have applicability to important applications such as optically limiting devices, multiphoton microscopy, carrier generation deep inside samples via nonlinear absorption,[38, 39] and two-photon three-dimensional lithography.[40]

ACKNOWLEDGMENTS

The W. M. Keck Foundation Free Electron Laser staff at Vanderbilt University and the Vanderbilt Institute for Nanoscale Science and Engineering are acknowledged. We thank Shekhar Guha and Joel Murray for valuable guidance, and John Kozub and Hernando Garcia for helpful

discussions. This research was supported by the National Science Foundation under grant NSF CHE□0707044.

REFERENCES

* Corresponding author. Email: picohen@umn.edu

[1]J. Bonse, G. Bachelier, J. Siegel and J. Solis, Phys. Rev. B **74**, 134106 (2006).

[2]B. Dragnea and B. Bourguignon, Phys. Rev. Lett. **82**, 3085 (1999).

[3]V. Recoules, J. Clerouin, G. Zerah, P. M. Anglade and S. Mazevet, Phys Rev Lett **96**, 055503 (2006).

[4]B. Koehler and S. George, Surface Science **248**, 158 (1991).

[5]M. Sheik□Bahae and H. Kwok, J. Appl. Phys. **63**, 518 (1988).

[6]D. M. Simanovskii, H. A. Schwettman, H. Lee and A. J. Welch, Phys. Rev. Lett. **91**, 107601 (2003).

[7]N. Zhang, X. Zhu, J. Yang, X. Wang and M. Wang, Phys. Rev. Lett. **99**, 167602 (2007).

[8]W. Roeterdink, L. Juurlink, O. Vaughan, J. Diez, M. Bonn and A. Kleyn, Applied Physics Letters **82**, 4190 (2003).

[9]K. Sokolowski-Tinten and D. von der Linde, Phys. Rev. B **61**, 2643 (2000).

[10]I. Zavestovskaya, P. Eliseev, O. Krokhin and N. Men'kova, Appl. Phys. A **92**, 903 (2008).

[11]H. Furuse, N. Mori, H. Kubo, H. Momose and M. Kondow, Journal of Materials Science: Materials in Electronics **18**, 81 (2007).

[12]A. Gibson, C. Hatch, P. Maggs, D. Tilley and A. Walker, J. Phys. C **9**, 3259 (1976).

[13]R. James, J. Appl. Phys. **54**, 3220 (1983).

[14]C. Rauscher and R. Laenen, J. Appl. Phys. **81**, 2818 (1997).

[15]D. Seo, L. Feldman, N. Tolk and P. Cohen, in *Laser-Induced Damage in Optical Materials: 2008*, Proc. SPIE **7132**, 713216 (2008).

[16]E. Tuncel, J. L. Staehli, C. Coluzza, G. Margaritondo, J. T. McKinley, R. G. Albridge, A. V. Barnes, A. Ueda, X. Yang and N. H. Tolk, Phys. Rev. Lett. **70**, 4146 (1993).

[17]T.J. Wagner, Ph.D. thesis, Air Force Institute of Technology, 2010.

[18]S. Yuen, R. Aggarwal and B. Lax, J. Appl. Phys. **51**, 1146 (1980).

[19]H. Furuse, N. Mori, H. Kubo, H. Momose and M. Kondow, Phys. Rev. B **74**, 205206 (2006).

[20]H. Furuse, N. Mori, H. Kubo, H. Momose and M. Kondow, Phys. Rev. B **75**, 205101 (2007).

[21]G. Edwards, D. Evertson, W. Gabella, R. Grant, T. King, J. Kozub, M. Mendenhall, J. Shen, R. Shores and S. Storms, IEEE Journal of Selected Topics in Quantum Electronics **2**, 810 (1996).

[22]J. Kozub, B. Feng and W. Gabella, in *Commercial and Biomedical Applications of Ultrafast and Free-Electron Lasers*, **4633**, 153 (2002).

[23]W. Kaiser, R. Collins and H. Fan, Phys. Rev. **91**, 1380 (1953).

[24]X. Q. Zhou, H. M. van Driel and G. Mak, Phys. Rev. B **50**, 5226 (1994).

[25]M. Levinshtein, S. Rumyantsev and M. Shur, *Handbook Series on Semiconductor Parameters* (World Scientific Publishing Company, 1996), Vol. 1 p. 218.

[26]E. Gaubas and J. Vanhellemont, Appl. Phys. Lett. **89**, 142106 (2006).

[27]D. Auston, C. Shank and P. Lefur, Phys. Rev. Lett. **35**, 1022 (1975).

[28]H. M. van Driel, L. Lompré and N. Bloembergen, Appl. Phys. Lett. **44**, 285 (1984).

[29]C. Cirloganu, P. Olszak, L. Padilha, S. Webster, D. Hagan and E. Stryland, Opt. Lett. **33**, 2626 (2008).

[30]B. Wherrett, JOSA B **1**, 67 (1984).

[31]E. W. Van Stryland, S. Guha, H. Vanherzeele, M. Woodall, M. Soileau and B. Wherrett, J. Mod. Opt. **33**, 381 (1986).

[32]S. Krishnamurthy, in *IR Materials Meeting 2010*, Dayton, OH, (2010).

[33]H. Garcia and R. Kalyanaraman, J. Phys. B **39**, 2737 (2006).

[34]R. Wenzel, G. Arnold and N. Greiner, Appl Opt **12**, 2245 (1973).

[35]L. Gonzalez, J. Murray, S. Krishnamurthy and S. Guha, Optics Express **17**, 8741 (2009).

[36]A. Bristow, N. Rotenberg and H. M. van Driel, Appl. Phys. Lett. **90**, 191104 (2007).

[37]D. Reitze, T. Zhang, W. Wood and M. Downer, JOSA B **7**, 84 (1990).

[38]J. Bhawalkar, G. He and P.N. Prasad, Reports on Progress in Physics **59**, 1041 (1996).

[39]D. Mcmorrow, W. Lotshaw, J. Melinger, S. Buchner and R. Pease, IEEE Transactions on Nuclear Science **49**, 3002 (2002).

[40]M. Farsari, B. Chichkov and N. Photonics, Nature Photonics **3**, 450 (2009).